Brain Struct Funct (2007) 212:37–54
DOI 10.1007/s00429-007-0142-4

ORIGINAL ARTICLE

Comparative analysis of extra-ventricular mitoses at early stages of cortical development in rat and human

Rosalind S. E. Carney · Irina Bystron · Guillermina López-Bendito · Zoltán Molnár

Received: 31 October 2006 / Accepted: 30 April 2007 / Published online: 2 June 2007
© Springer-Verlag 2007

Abstract Embryonic germinal zones of the dorsal and ventral telencephalon generate cortical neurons during the final week of gestation in rodent and during several months in human. Whereas the vast majority of cortical interneurons originate from the ventral telencephalon, excitatory neurons are locally generated within the germinal zone of the dorsal telencephalon, the future cerebral cortex, itself. However, a number of studies have described proliferating cells external to the ventricular and subventricular germinal zones in the developing dorsal telencephalon. In this study, we performed a comprehensive cell density analysis of such 'extra-ventricular proliferating cells' (EVPCs) during corticogenesis in rat and human using a mitotic marker anti-phospho-histone H3. Subsequently, we performed double-labelling studies with other mitotic and cell type specific markers to undertake phenotypic characterisation of EVPCs. Our findings show: (1) the densities of extra-ventricular H3-positive ($H3^+$) cells were surprisingly similar in preplate stage rat and human; (2) extra-ventricular proliferation continues during mid-and late corticogenesis in rat and in early fetal human cortex; and (3) extra-ventricular cells appear to be mitotic precursors as they are not immunoreactive for a panel of early post-mitotic and cell type-specific markers, although (4) a subset of EVPCs are proliferating microglia. These data suggest that some aspects of early corticogenesis are conserved between rodent and human despite marked differences in the duration of neurogenesis and the anatomical organisation of the developing cerebral cortex.

Keywords Cerebral cortex · Development · Immunohistochemistry · Proliferation · Rodent · Primate

Electronic supplementary material The online version of this article (doi:10.1007/s00429-007-0142-4) contains supplementary material, which is available to authorized users.

R. S. E. Carney · I. Bystron · G. López-Bendito · Z. Molnár (✉)
Department of Physiology, Anatomy & Genetics, University of Oxford, South Parks Road, Oxford OX1 3QX, UK
e-mail: zoltan.molnar@anat.ox.ac.uk

I. Bystron
Department of Morphology, Institute of Experimental Medicine, 12 Acad. Pavlova, St Petersburg 197376, Russia

Present Address:
R. S. E. Carney
Center for Neuroscience Research, Suite 5340, Children's Research Institute, Children's National Medical Center, Washington, DC 20010, USA

G. López-Bendito
Instituto de Neurociencias de Alicante, CSIC & Universidad Miguel Hernández, 03550 San Joan d'Alacant, Spain

Introdcution

In the mammalian neocortex, cortical neurons are generated in germinal zones of the embryonic telencephalon and migrate to their ultimate laminar and areal destination in the mature brain (Angevine and Sidman 1961). In rodents, cortical projection neurons are produced during a 6-day corticogenetic period in the pallial germinal zone (GZ), which consists of two progenitor compartments. The ventricular zone (VZ) lies adjacent to the ventricular surface and is characterized by the interkinetic migration (IKM) of its precursors, which places mitotic cells apically and S-phase cells in the basal portion of the VZ (Sauer 1935a; Sauer and Walker 1959). The subventricular zone (SVZ), appears later in development and those cells do not un-

dergo IKM (Boulder Committee 1970). Lamination of the cortical neuroepithelium results in the accumulation of the first population of post-mitotic neurons from the VZ subjacent to the pial surface, and the formation of the primordial plexiform layer (Marin-Padilla 1971; Meyer et al. 1998), early marginal zone (Rickmann et al. 1977; Raedler and Raedler 1978) or preplate (Stewart and Pearlman 1987), although in human, the first neurons of the preplate (PP) invade the cortex from subpallial sources (Bystron et al. 2006). The preplate is subsequently split into a deep subplate (SP) and superficial marginal zone (MZ, future layer I) by the neurons of the developing cortical plate (CP) proper (Marin-Padilla 1971 1972; Luskin and Shatz 1985). Formation of the cortical plate occurs in a chronologically ordered sequence with young neurons migrating past their older counterparts forming the cortical layers VI-II in an 'inside-out' fashion (Angevine and Sidman 1961; Berry and Rogers 1965).

Gliogenesis commences during late corticogenesis and continues perinatally in the SVZ (Privat 1975) and hence neurogenesis and gliogenesis were thought to occur in the VZ and SVZ, respectively (Angevine and Sidman 1961; Sturrock and Smart 1980). However, the appearance of 'non-surface' (SVZ) mitoses (Smart 1985), SVZ expansion during corticogenesis and thymidine labelling studies lead to the suggestion that cortical layers IV–II were produced by the SVZ in rodent (Smart and McSherry 1982).

Concomitant to these developments in the understanding of the role of the SVZ in corticogenesis were important discoveries in the VZ. It is now known that radial glia (RG) are the primary precursor cell type of the ventricular zone (Malatesta et al. 2000; Noctor et al. 2001; Tamamaki et al. 2001; Gal et al. 2006). Using Tis21-GFP mice, in which all neuron-producing progenitors are revealed, a population of neurogenic progenitors in the basal portion of the VZ has been described (Haubensak et al. 2004). Whereas it has been assumed that the cells of the VZ set up the SVZ (Smart and McSherry 1982) this has not been definitively demonstrated. Nonetheless, these compartments share an intricate relationship as described recently in time-lapse microscopic studies. It has been shown that cortical neurons can arise directly from radial glia in the VZ or indirectly from 'intermediate progenitor cells' (IPCs or 'basal progenitors') in the SVZ (Noctor et al. 2004; Haubensak et al. 2004; Miyata et al. 2004).

While the RG and IPCs of the VZ and SVZ, respectively, are undoubtedly responsible for generating the overwhelming majority of cortical neurons, cell proliferation external to the GZ has been described in several studies. An extra-germinal source of precursor cells has been suggested in the PP (Valverde et al. 1995), intermediate zone (IZ, Smart 1973; Kamei et al. 1998; Levers et al. 2001) and the SP, CP and MZ in rodent cortex (Levers et al. 2001). In the developing neocortex, the transcriptions factors Pax6, Tbr2 and Tbr1 are expressed sequentially by radial glia, IPCs and lastly post-mitotic neurons, respectively (Hevner et al. 2006). Expression of Pax6 and Tbr2 was occasionally noted in cells external to the germinal zones in superficial compartments, such as the IZ, SP and CP (Englund et al. 2005). Similarly, proliferating cells external to the GZ in developing human dorsal telencephalon have been described using a variety of histological and immunohistochemical techniques (Kendler and Golden 1996; Zecevic 2004; Bystron et al. 2006). In this study, we assessed the extent of such 'extra-ventricular proliferating cells' (EVPCs) that occur external to the VZ and SVZ compartments of the dorsal telencephalic germinal zone, in both rat and human cortex.

Materials and methods

Brain specimens

Wistar rats were maintained on a standard diet and light cycle and were mated in the Departmental Animal Colony in the University of Oxford, UK. The day of plug detection was defined as embryonic day 0 (E0). Time-mated pregnant females were killed by cervical dislocation and the embryos harvested by Caesarean section. The embryos were decapitated and the heads were post-fixed overnight in 4% paraformaldehyde in 0.1 M phosphate buffer, pH 7.4 (4% PFA in PB 0.1M) at 4°C. All experimentation was approved by, and in accord with, the regulations and guidelines of the Home Office (United Kingdom) and the University of Oxford. We obtained human embryos and early fetuses after legal abortions at the St. Petersburg Centre of Family Planning and Reproduction, following national ethics guidelines in Russia, in accord with the recommendations of the Polkinghorne report (1989). Human embryogenesis is conventionally described in terms of Carnegie Stages (CS), on the basis of several morphological criteria (O'Rahilly 1999; Bystron et al. 2006). The whole embryos and brains were fixed in 4% PFA for 7–10 h with minimal post-mortem delay. Embryos from E12.5 and E15.5 Tis21-GFP mice, harvested as described above for rat, were kindly provided by Dr. Wieland Huttner (Max Planck Institute, Dresden, Germany).

Immunohistochemistry

For the quantitative analysis, H3 immunohistochemistry was used as a marker of mitotic cells (Estivill-Torrus et al. 2002). For rat, the brains were dissected from the head before embedding in 4% agarose (4% agar) in phosphate buffered saline (PBS; 0.1M phosphate buffer;

0.09% NaCl, pH 7.4). The pia and mesenchyme (referred to collectively as mesenchyme; ME), external to the cortex, were not removed during dissection to avoid damaging the cortex. Coronal sections at a thickness of 50 μm were prepared using a Vibroslicer (Leica VT1000S). Standard immunohistochemical protocols were used. To block non-specific binding sites, free-floating sections were incubated in 10% normal goat serum (NGS) diluted in Tris-buffered saline (TBS; 50 mM Tris buffer, 0.09% NaCl, pH 7.4) with 0.3% Triton (TBST 0.3%) to increase antibody penetration. Antibodies were diluted in 1% NGS in TBS and 3 × 10 min rinses in TBS were carried out between each step. The sections were incubated overnight at 4°C in rabbit polyclonal anti-phosphohistone H3 antibody (1:500, Upstate Biotechnology) prior to incubation in the Cy3 secondary antibody (1:500, Jackson Immunoresearch) for 2 h at RT. The sections were counterstained with the fluorescent DNA dye, bisbenzimide (2.5 μg/ml in PBS, Sigma) for 10 min at RT, before final rinses in TBS. The sections were mounted on glass slides and coverslipped with PB:glycerol (1:1). Negative controls with omission of either primary antibody but both secondary antibodies only showed immunoreactivity with the appropriate fluorochrome (not shown). For human tissue, the same protocol was used with the exception that the whole head was embedded in 4% agar sectioned coronally at a thickness of 70 μm. For sections that were co-immunolabelled with mouse monoclonal anti-phosphorylated vimentin (4A4; 1:2,000, Stratech), incubation in biotinylated goat anti-mouse antibody (1:100, Vector Labs), was required prior to incubation with the fluorochromes, Cy2-conjugated streptavidin and goat anti-rabbit Cy3 to visualise 4A4 and H3, respectively.

For additional double-labelling experiments the following antibodies were used: mouse monoclonal anti-beta tubulin III (TUJ1; Abcam, 1:1,000), human neuronal protein HuC/HuD monoclonal antibody 16A11 (Hu; Molecular Probes, 1:1,000), mouse monoclonal anti-Reelin (Chemicon, 1:2,000), rabbit polyclonal anti-Tbrain1 (Tbr1; 1,000, kind gift from Dr. R. Hevner), rabbit polyclonal anti-calbindin (Swant, 1:2,000), rabbit polyclonal anti-calretinin (Swant, 1:2,000), polyclonal anti-GABA (Sigma, 1:5,000), polyclonal rabbit anti-pan-Dlx antibody (Dll; 1:75, kind gift from Dr. J. Kohtz), polyclonal NG2 chondroitin sulfate proteoglycan antibody (NG2; Chemicon, 1:200) and biotinylated lectin *Riccinis communis agglutinis* (RCA-1; Vector Laboratories, 1:1,000).

Additionally, cortical H3 immnoreactivity in multiple sections from Tis21-GFP mice (n = 3 brains at both E12.5 and E15.5) was analysed. Examination of intrinsic Tis21-GFP fluorescence and H3 immunolabelling was performed using epifluoresence microscopy, throughout the z-plane of the section. Areas of potential co-expression were further analysed by confocal microscopy and individual optical sections and collapsed projection images were analysed.

Cell quantification and co-immunolabelling analysis

Rat embryos at E13, E15, E17, and E19 (n = 8 for each stage, all littermates) and PP stage human (Carnegie Stage [CS] 16–20, embryonic days 37–39 to 47–49 [E37–39 to E47–49]; n = 9 brains) were used for quantification. Additional human brains at fetal ages 9–10, and 11–12 gestational weeks (GW, both n = 1) were processed for H3 (11–12 GW) and H3/4A4 (8–9 GW) but not included in the quantitative analysis (all numbers and ages of human brains used are listed in Table 1). Prior to analysis, the sections were examined by fluorescence microscopy, focussing throughout the z-plane of the tissue to ensure full antibody labelling of the tissue to exclude sections with insufficient labelling from the study. Cell quantification was carried out using fluorescence microscopy with an ocular reticule of 66,000 μm^2 area under a ×40 objective lens which was placed always perpendicular to the ventricular surface. The number of $H3^+$ cells in each anatomical compartment i.e. VZ, SVZ, IZ, SP, CP, MZ, PP, was counted by focussing up and down in the z-plane of the section. Cortical histogenesis proceeds along rostro-caudal and lateral-medial gradients (Angevine and Sidman 1961; Smart and Smart 1977; Bayer and Altman 1991), hence cell quantification was performed in rostral, intermediate and caudal cortical sections (Fig. 1A), and in two locations within the pallium; 'lateral' and 'medial', corresponding to dorsolateral and dorsomedial cortex, respectively (Fig. 1B). One littermate brain per age was sectioned and stained for cresyl violet using standard protocols as described elsewhere (Jones et al. 2002) for anatomical

Table 1 Numbers and developmental stages of human embryos and fetuses used in this study

Period	Age (Carnegie stage [CS]/gestational weeks [GW])	Number of brains processed	Immunohistochemical labelling
Embryonic (total n = 9)	CS 16	2	H3
	CS 17–17.5	3	H3 (CS 17) H3/4A4 (CS 17.5)
	CS 18	1	H3
	CS 19–20	1	H3
	CS 20	2	H3
Early fetal (total n = 2)	9–10 GW	1	H3/4A4
	11–12 GW	1	H3

Details of human brains processed immunohistochemically for anti-phospho-histone H3 (H3) and anti-phosphorylated vimentin (4A4) are given in the right-hand column

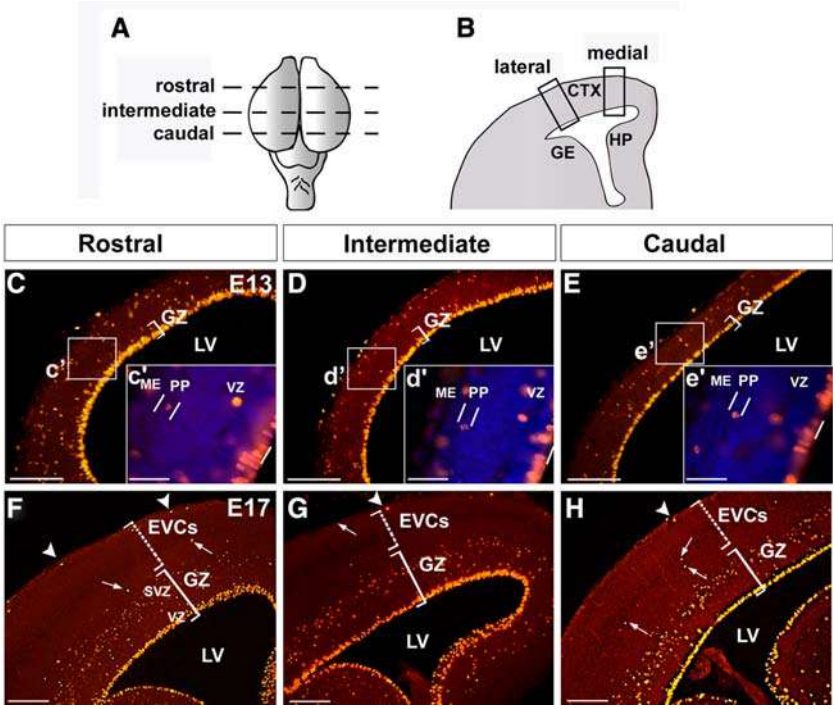


Fig. 1 H3 immunolabelling reveals mitotic cells in anatomical compartments external to the germinal zone during rat corticogenesis. **A**, **B** Schematic diagrams showing the rostro-caudal axis and lateral and medial locations where cell quantification was carried out. Representative coronal sections from rostral (**C**, **F**), intermediate (**D**, **G**) and caudal (**E**, **H**) cortical regions of embryonic day (**E**) 13 and E17 brains anti-phospho-histone H3 (H3; *red*). At E13, the majority of H3-immunopositive ($H3^+$) cells were in the ventricular zone (VZ) of the germinal zone (GZ, bracket), although a number of $H3^+$ cells were located in the preplate (PP) as shown in high-power insets (*c′–e′*). At E17, in addition to the VZ, a band of $H3^+$ cells constituted the mitotic cells of the subventricular zone (SVZ) (**F**–**H**). Scattered $H3^+$ cells were also found in the 'extraventricular compartments' (EVCs) (**F**–**H**, *arrows*) external to the GZ. $H3^+$ cells located in the EVCs are referred to as 'extra-ventricular proliferating cells' (EVPCs) in the present study. Proliferating mesenchymal cells were also $H3^+$ (**F**–**H**, *arrowheads*). Abbreviations: *CTX* cortex; *HP* hippocampus; *GE* ganglionic eminence; *LV* lateral ventricle. Scale: **C**–**H**: 200 μm, **L**–**N**, *c′–e′*: 50 μm

comparison of cortical wall development. Three sections for each rostral, intermediate or caudal location were used and quantification was carried out in both hemispheres yielding $n = 48$ for each observation overall. Quantification preceded data analysis to exclude bias by the observer.

The average number of $H3^+$ cells in each sampling area was calculated for each rat at each development stage, and the corresponding values from all eight littermates were used to estimate mean and SEM values. There was no obvious variation in the size of the littermate brains therefore, the thickness of each cortical compartment was measured in each cortical region and latero-medial location in one representative brain for each age. The average cortical thickness (expressed in millimetres) was measured in digital images of bisbenzimide counterstaining at each developmental stage and always measured from the VZ to the pial surface. Cortical thickness was measured in a similar manner in human specimens. The average $H3^+$ cell density in each cortical compartment was calculated by multiplying the mean number of $H3^+$ cells by the thickness (μm) of the cortical compartment, divided by the total thickness of the cortical wall, which was measured (μm) for each sampling region at each developmental stage. Quantification of cell densities was expressed per mm^3 of cortical surface area by multiplying the average $H3^+$ cell density per the thickness of the section (50 μm in the case of rat slices and 70 μm in the case of human tissue). The average $H3^+$ cell density in each anatomical compartment is visualized as histograms (Fig. 2A–D). In addition, the average $H3^+$ cell density in the entire cortical wall (i.e. combined average of anatomical compartments) per sample is indicated by a dashed black line (Fig. 2A–D).

Anatomy and nomenclature

In the current study we used the nomenclature as described by the Boulder Committee (1970). In the ventricular zone, cells undergo 'interkinetic nuclear migration' (IKM) whereby mitosis occurs at the ventricular surface. In contrast, the SVZ is the architectonic region between the VZ and IZ in which the cells do not display IKM and therefore divide in situ. Takahashi and colleagues (1995) previously

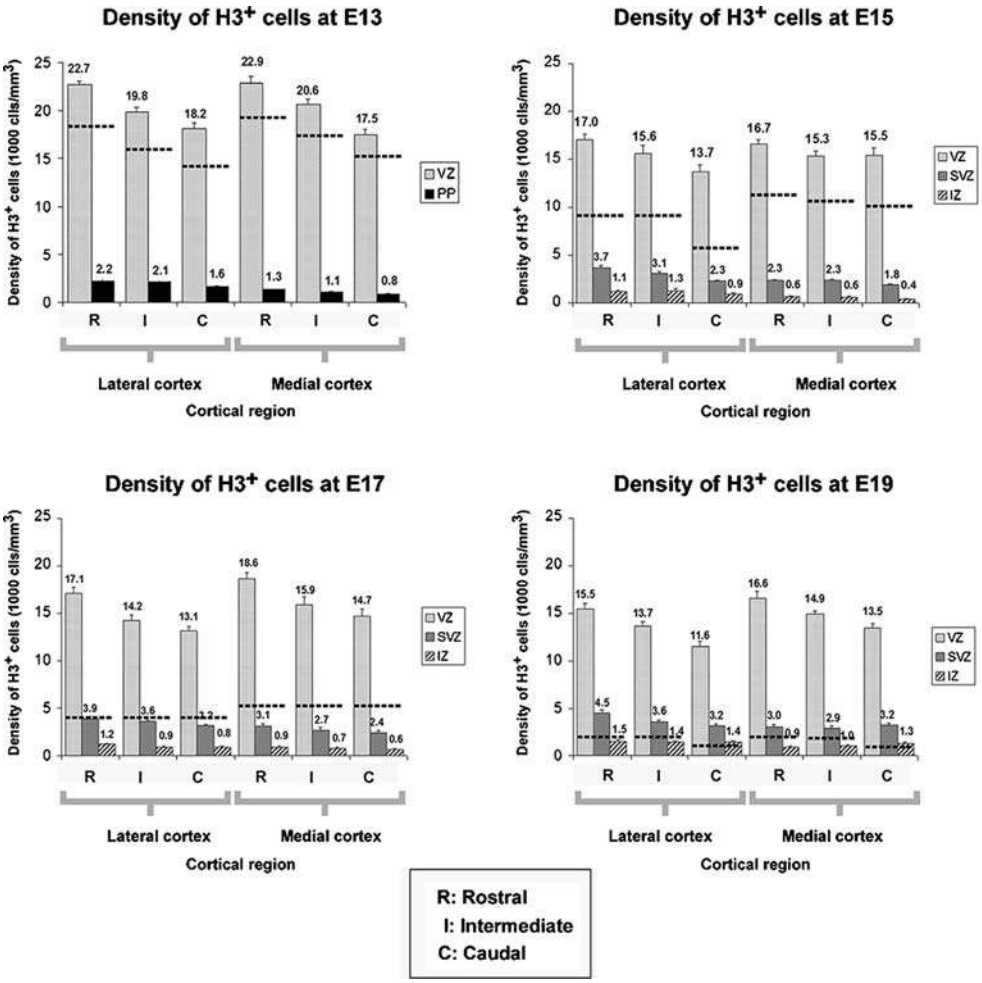


Fig. 2 Density of $H3^+$ cells per mm^3 cortical surface during corticogenesis in rat Density of $H3^+$ cells (1,000 cells per mm^3 cortical surface) throughout corticogenesis in rat (E13–E19). Data are expressed as mean ± SEM, mean values are given above each column and dashed black lines indicate the average $H3^+$ cell density in that column. **A** At E13, both lateral and medial cortex showed rostro-caudal gradients of proliferation in the VZ (*grey speckled*) and PP (black). Density of $H3^+$ cells in the VZ, SVZ (*dark grey*), intermediate zone (IZ, *striped*) at E15 (**B**), E17 (**C**) and E19 (**D**). At all these ages, rostro-caudal gradients of proliferation were observed in the VZ, SVZ and IZ. In all developmental stages, mitotic activity was more predominant in medial than lateral cortex. $H3^+$ EVPCs were also present in the SP and CP at E15 (lateral cortex), E17 and E19 (values given in main text) but not the MZ. At all stages of corticogenesis, a higher density of mitotic cells was observed in medial compared with lateral cortex

described a secondary proliferative population (SPP), which arises from the primordial pseudostratified ventricular epithelium, corresponding to the SVZ and VZ regions as defined by the Boulder Committee (1970). Takahashi and colleagues (1995) included some proliferative cells in the upper IZ (Takahashi et al. 1995) as part of the SPP. However, as other studies have noted cell proliferation in more superficial compartments, i.e. SP and CP, we concluded that in this study, the IZ should be considered as a separate anatomical compartment from the SVZ proper. For lower-power images we have used the term 'extraventricular compartments (EVCs) to indicate the anatomical compartments of the cortical wall that are external to the VZ/SVZ.

Data analysis

Digital photographs were obtained with a Leica DC500 camera, using conventional fluorescence microscopy, and selected regions were also imaged on a laser scanning confocal microscope (Leica TCS SP1). All images were reconstructed, and the images obtained with different filters merged, using Adobe Photoshop 6.0 software. Adjustments to colour and/or contrast were applied across each image as a whole.

Results

Patterns of H3 immunolabelling and quantification of $H3^+$ cell density during corticogenesis in rat

H3 immunolabelling was used for quantitative analysis of mitotic cell density during development in rat and human. H3 immunoreactivity was nuclear and predominantly occurred in mitotic cells, although a minority of G2 phase cells was labelled. Cells in G2 phase and cells expressing H3 very weakly, the latter occurring primarily in the SVZ at E17/E19 only, were excluded from the analysis. Cortical anatomical compartments were revealed by bisbenzimide counterstaining and by comparison to a littermate brain stained with cresyl violet (not shown). In E13 rat, the cortical wall was bilaminate and consisted of the VZ and PP in both lateral and medial cortex at all rostro-caudal

levels. At E13 and E17 (Fig. 1C–E and F–H), the majority of $H3^+$ cells were located at the apically in the VZ and at E17, mitotic cells of the SVZ appeared as a band of $H3^+$ cells superficial to the VZ. $H3^+$ cells were also observed external to the germinal zone in the PP at E13 (Fig. 1c′–e′) and in the compartments external to the GZ in the cortical wall at E17 (Fig. 1F–H), constituting the extra-ventricular proliferating cells of the current study. Proliferating mesenchymal cells outside the cortex were also $H3^+$ (Fig. 1F–H).

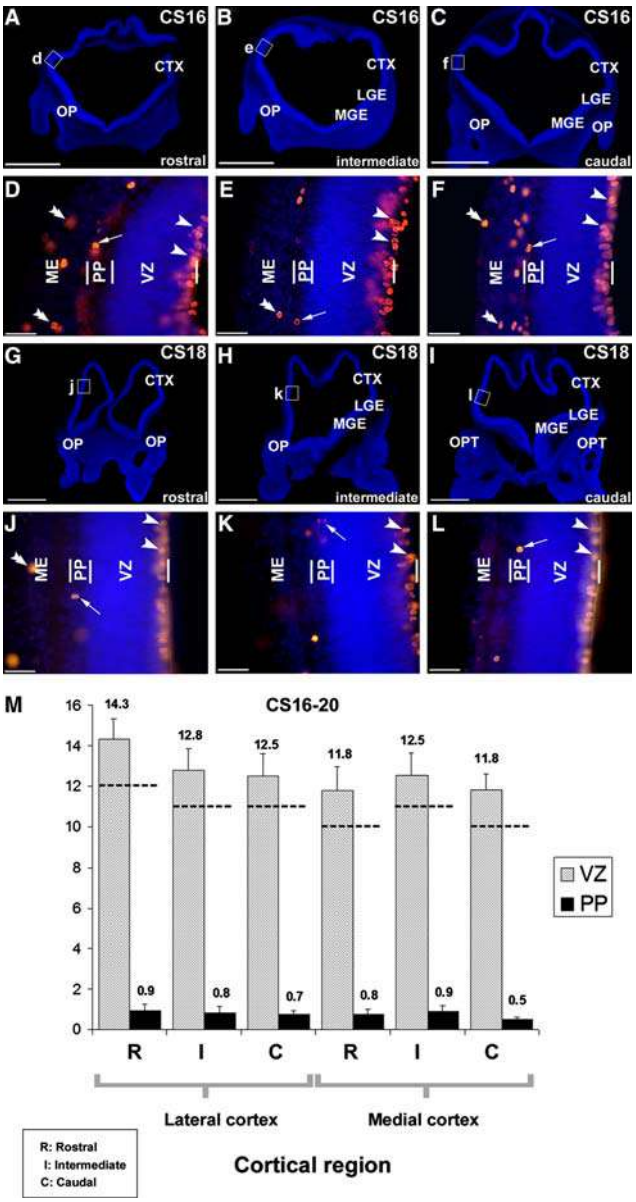
To determine the significance of EVPCs during rat corticogenesis, the density of $H3^+$ cells in the cortical wall was quantified at 4 developmental stages (E13–E19; Fig. 2A–D). A total of 75,835 $H3^+$ cells were counted; 21,025 (E13), 18,155 (E15), 18,638 (E17) and 18,017 (E19). All at ages, mitotic activity, evidenced by $H3^+$ immunoreactivity decreased in a rostro-caudal gradient, and in medial cortex, the density of mitotic cells exceeded that in lateral regions. At E13, we estimated the occurrence of EVPCs ($H3^+$ cells in the PP; Fig. 2A) to represent 7.55% (~1,531/20,280 cells/mm^3) of the total $H3^+$ population in the cortical wall. Compared to the VZ $H3^+$ cell density, more $H3^+$ cells were in the PP of lateral (9.84%; ~1,191/20,236 cells/mm^3) than medial cortex (5.27%; ~1,071/20,324). At E15, the major histogenetic change has taken place with the emergence of the CP in lateral regions, which tapered off medially where the PP remained. The SVZ was present in throughout the ventro-medial extent of the cortical wall, though no CP was detected medially. The density of $H3^+$ cells in the SVZ comprised 19% (~3,011/15,455 cells/mm^3) and 14% (~2,180/15,823) of the $H3^+$ cells in the VZ, in lateral and medial cortex, respectively. $H3^+$ cells were present in the IZ at E15 (Fig. 2B) and also in the PP in medial cortex, which from E13 had decreased dramatically to constitute 0.59% of $H3^+$ cells in the VZ (~93/15,823 cells/mm^3). Concurrent with the appearance of the CP, the PP has been split into a superficial MZ and deep SP. The apical and basal limits of the SVZ were easily distinguishable by H3 immunoreactivity, which labelled the mitotic cells that divide in situ as IKM does not occur in this compartment. At E15, E17 and E19 (Fig. 2B–D), similar proliferative gradients were observed in the VZ, SVZ and IZ, with medial and rostral cortical regions exhibiting the highest density of $H3^+$ cells. In addition, $H3^+$ cells were observed in the SP and CP but not the MZ from E15–E19. Although present, the low densities of EVPCs in the SP and CP precluded these data being depicted graphically with the GZ/IZ densities. Instead, to give a clearer picture of the extent of EVPC density throughout development, combined percentage values of $H3^+$ EVPCs in the IZ, SP and CP with respect to the GZ $H3^+$ cell density were determined separately for lateral and medial cortex from E15–E19, and data for total cell numbers are included. At E15, the proportion of $H3^+$ cells in extra-ventricular compartments was similar in lateral and medial cortex. EVPCs in the IZ, SP and CP in lateral cortex comprised 3.05% (~281/9,233) of GZ $H3^+$ cells. In medial cortex, $H3^+$ cells in the PP and IZ represented 3.39% (~305/9,001) of $H3^+$ cell density in the GZ. At E17, lateral EVPCs accounted for 2.73% (~251/9,178) of $H3^+$ cell density in the GZ, and medially this estimate was 1.97% (~189/9,573). Akin to earlier developmental stages, at E19, the percentage of EVPCs compared to $H3^+$ cell density in the GZ was more prominent laterally (4.81%; ~417/8,668) than medially (3.36%; ~303/9,012). Therefore, for the most part, EVPC density showed a general lateral to medial developmental gradient. Overall, the density of EVPCs decreased rostrally to caudally at all ages with two main exceptions: a peak of $H3^+$ cell density in intermediate lateral cortex at E15 and a high caudal to low rostral gradient of EVPC density in medial cortex at E19.

Patterns of H3 immunolabelling during preplate stage in human cortex

Quantification of $H3^+$ cell density was carried out in preplate stage human brains ($n = 9$), which ranged from CS 16–20 and a total of 5,464 $H3^+$ cells were counted. We observed extra-ventricular $H3^+$ cells in the preplate from CS 16–20 in all rostro-caudal and dorso-lateral cortical regions (Fig. 3D–F and J–L for CS 16 (E37–39) and CS 18 (E42–43), respectively). $H3^+$ cells were also observed in the mesenchyme, external to the developing cortical wall. Cell quantification demonstrated that in both the VZ and PP in lateral cortex, the density of $H3^+$ cells decreased rostrally to caudally, whereas in medial cortex, intermediate cortical regions showed the highest frequency of mitotic cells (Fig. 3M). Nonetheless, the density of $H3^+$ cells in the PP reflected the relative gradient of that in the VZ, showing a rostro-caudal and high intermediate, rostral to low caudal gradient in lateral and medial cortex, respectively. EVPCs in the PP comprised 6.19% (~782/12,630 cells/mm^3) of the total $H3^+$ cells in the cortical wall, and, similar to rodent, showed a predominance in lateral cortical regions; 6.37% lateral (~842/13,219), 5.99% (~722/12,041) medial.

Examination of phosphorylated vimentin expression in extra-ventricular proliferating cells in rat and human cortex

We next examined phosphorylated vimentin, 4A4, immunoreactivity in EVPCs in both rat and human cortex. In rat cortex during development, we found that 4A4 immunoreactivity was present in three categories of cells: (1) $4A4^+$ cells in the GZ (RG and IPCs); (2) $4A4^+$ cells located



◀ **Fig. 3** Distribution pattern of $H3^+$ cells and density per mm^3 of cortical surface during early human embryonic cortical development. Rostral (**A**,**G**), intermediate (**B**,**H**) and caudal (**C**,**I**) coronal sections of Carnegie Stage (CS) 16 embryonic days 37–39 (E37–39; **A**–**C**) and CS 18 (E42–43; **G**–**I**) human cortex (CTX), stained with bisbenzimide (*blue*) to reveal anatomical structures. **D**–**F**, **J**–**L** Higher-power views of the areas boxed in **A**–**C** and **G**–**I**, respectively, showing the distribution of $H3^+$ cells (*red*), and the cortical compartments revealed by bisbenzimide counterstaining. As expected, most of the $H3^+$ cells were located apically in the ventricular zone (VZ, *arrowheads*). However, extra-ventricular proliferating $H3^+$ cells were also observed in the preplate (PP, *arrows*) in all rostro-caudal cortical regions at both stages. Mitotic cells in the mesenchyme (ME) were also observed (**D**–**F**, **J**, *double arrowheads*). **M** Density of $H3^+$ cells (1,000 cells per mm^3 cortical surface) during the PP stage (CS 16–20; E37–39 to E47–49) in human cortex. Data are expressed as mean ± SEM, mean values are given above each column and *dashed black lines* indicate the average $H3^+$ cell density in that column. In lateral cortex, both the VZ (*grey speckled*) and PP (*black*) showed a rostro-caudal gradient of $H3^+$ cell density in both the VZ and PP. In medial cortex more $H3^+$ cells occurred in intermediate cortical regions than elsewhere for both the VZ and the PP. Abbreviations: *OPT* optic vesicle, *OP* olfactory placode, *LGE* lateral ganglionic eminence, *MGE* medial ganglionic eminence. Scale bars: **A**–**C**, **G**–**I**: 1 mm, **D**–**F**, **J**–**L**: 50 μm

external to the GZ that are mostly devoid of processes (EVPCs) and (3) $4A4^+$ cells located within or in close proximity to brain vasculature. The latter tended to have weaker immunoreactivity, were oval in morphology and occurred in groups and so were easily distinguishable from the individual, round $4A4^+$ cells, located distal to blood vessels that were the primary concern of this study. Moreover, both the bisbenzimide counterstaining and the 4A4 immunostaining of the blood vessels themselves clearly delineated the brain vasculature.

As described previously, 4A4 immunoreactivity labels mitotic GZ precursors with occasional labelling of pial-directed processes. Interestingly, we observed 4A4 expression in the majority of EVPCs in all anatomical compartments throughout corticogenesis. Whereas, infrequent pial-directed processes were observed from $4A4^+$ RG in the VZ, the vast majority of $4A4^+$ EVPCs lacked evident pial-directed processes, with the only exceptions observed during the terminal stage of corticogenesis, at E19 (see Fig. 5N, P, R). $H3^+/4A4^+$ cells were initially observed in the PP at E13, the earliest stage examined, independent of cortical region or medial or lateral anatomical location (not shown). At E15, double-positive cells were observed in the remaining PP and the IZ in medial cortex (Fig. 4G–I) and in the IZ in lateral cortex (Fig. 4D–F), in addition to the GZ, in all rostro-caudal cortical regions. It is important to note that EVPCs in the IZ did not seem to merely represent 'displaced' SVZ cells as they were observed in both apical and basal portion of this zone. At E17, $H3^+$ cells were found in the IZ and in the SP and CP (Fig. 5A–F), although none were observed in the MZ. Many of the $H3^+$ cells in the IZ, SP and CP were also $4A4^+$ (Fig. 5a′–f′). At E19, $H3^+$ cells were present in the IZ, SP and CP (Fig. 5G–L), and the majority were also $4A4^+$ (Fig. 5M–R). At E19, in contrast to earlier developmental stages, some EVPCs displayed short $4A4^+$ processes that extended in the direction of the pial surface (Fig. 5N, P, R).

The mitotic markers H3 and 4A4 also label RG in human tissue (Weissman et al. 2003; Bystron et al. 2006). Here, double immunofluorescence in CS 17 (E40–41) cortex also demonstrated 4A4 colocalisation in $H3^+$ cells located in the VZ. Colocalisation of H3 and 4A4 in the PP was observed in all rostro-caudal cortical regions (Fig. 6D–F) and colocalisation of both markers was confirmed by confocal microscopy (Fig. 6G–I). As in rodent,

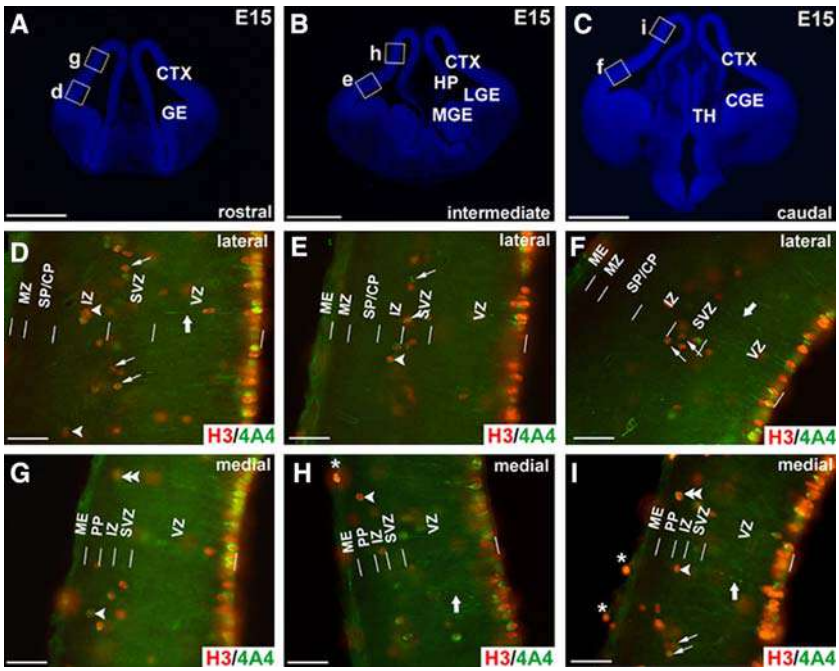


Fig. 4 Extra-ventricular proliferating cells are immunopositive for phosphorylated vimentin, 4A4, at mid-corticogenesis and early preplate. Representative rostral (**A**), intermediate (**B**) and caudal (**C**) coronal sections of an embryonic day 15 (E15) rat brain showing the cytoarchitectonic areas revealed by bisbenzimide staining (*blue*). **D–F** High-power views of the lateral areas boxed in **A–C**, respectively, showing the expression of H3 (*red*) and anti-phosphorylated vimentin (4A4; *green*) under double-exposure fluorescence microscopy. The majority of the $H3^+$ cells were also $4A4^+$ in the apical VZ and the SVZ. Double-positive cells were also located in the intermediate zone (IZ, *arrowheads*). Several 4A4-positive processes that extended radially towards the pial surface (**D**, **F**; *thick arrows*) were observed. **G–I** High-power views of the medial areas boxed in **A–C**, respectively, showing the expression of H3 and 4A4. As in lateral cortex, the majority of the $H3^+/4A4^+$ cells were located in the VZ, although the $H3^+$ cells in the preplate (PP, *double arrowheads*) and IZ (*arrowheads*) were also $4A4^+$. Labelled processes extended from VZ $4A4^+$ cells to the pial surface (**H**, **I**; *thick arrows*). Proliferating cells were also present external in the mesenchyme (ME) external to the cortical wall (**G**, **I**; *asterisks*). *CP* cortical plate, *MZ* marginal zone, *SP* subplate. Scale bars: **A–C**: 1 mm, **D–I**: 50 μm

$4A4^+$ cells in the human PP did not display any evident pial-directed processes. However, our examination of CS 17 human cortex did reveal occasional $4A4^+$ pial-directed processes from RG (see Fig. 6H), suggesting that the scaffold for radial migration of cortical neurons is present at this developmental stage.

In human, the early fetal period commences at 8 GW. At 9–10 GW, most of the $H3^+/4A4^+$ cells were present in the VZ and SVZ, however a small number of cells were present in IZ and subplate (Fig. 6J–L) similar to rodents. However, at 11–12 GW, the occurrence of $H3^+$ cells in extra-ventricular compartments had increased. $H3^+$ cells were observed in all apico-basal portions of the IZ, SP and CP (Fig. 6M–R). In contrast to rodent, we observed $H3^+$ cells in CP–MZ interface and in the MZ (Fig. 6Q, R). $H3^+$ cells in the human MZ were also $4A4^+$ (not shown).

Extra-ventricular proliferating cells do not express markers indicative of neuronal phenotypes

Having described the developmental distributions of EVPCs during rodent corticogenesis and in human preplate, we postulated that EVPCs may represent: 1) post-mitotic cells that have re-entered the cell cycle or 2) precursor cells which have not undergone prior terminal division. In order to address this, a panel of cell type-specific markers was combined with polyclonal H3 or monoclonal 4A4 mitotic markers in co-expression studies in early and late stage rat cortex. Antibodies that label newly post-mitotic cells included: anti-TUJ1, anti-HU, anti-Tbr1, anti-Reelin (see references below). At E14, TUJ1 immunoreactivity visualized the first population of post-mitotic neurons that accumulated and extended horizontal processes within the PP (Lee et al. 1990; Menezes and Luskin 1994) but none of PP cells co-expressed the mitotic marker H3 (Suppl. Fig. 1A–C). The anti-human neuronal protein HuC/HuD mouse monoclonal antibody 16A11 (anti-Hu) is detected as early as the neurons exit the cell cycle (Miyata et al. 2001). In E13 rat PP, Hu immunostaining appeared diffuse and did not appear to colocalize with H3 in non-surface mitoses as observed previously in E13 mouse (Miyata et al. 2004) (Suppl. Fig. 1D–F), although this may represent a species difference in antibody labelling or technical differences. Tbr1, a member

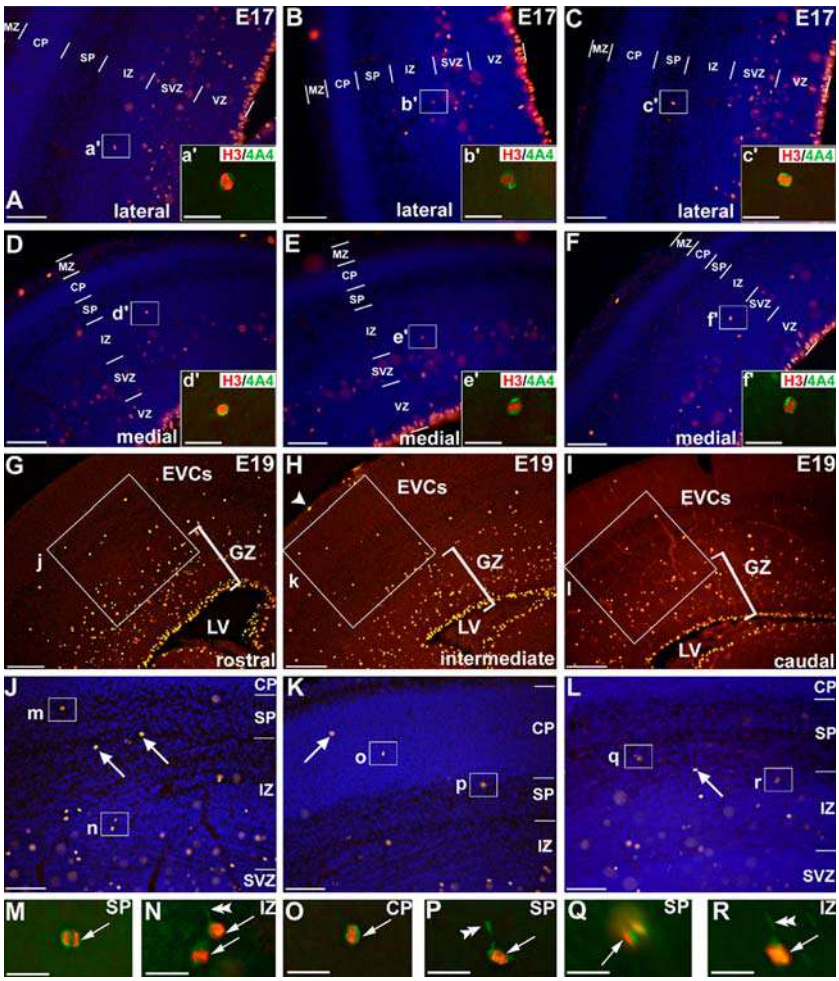


Fig. 5 Extra-ventricular proliferating cells are immunopositive for phosphorylated vimentin, 4A4 at mid- to late-corticogenesis. Overlay of H3 immunolabelling and bisbenzimide counterstaining of lateral (**A**–**C**) and medial (**D**–**F**) cortex at E17, in rostral (**A**, **D**), intermediate (**B**, **E**) and caudal (**C**, **F**) cortical regions. Mitotic cells were observed not only in the VZ and SVZ (**A**–**F**) but also in the IZ and subplate (SP) (*boxes* in **A**–**F**) and these cells were also immunopositive for 4A4 (*a′*–*f′*). **G**–**I** H3 immunoreactivity during the terminal phase of corticogenesis at E19. At E19, more $H3^+$ cells were found in extraventricular compartments such as the IZ, SP and cortical plate (CP) but no $H3^+$ cells were observed in the MZ. Proliferating cells in the ME were observed (**H**, *arrowhead*). $H3^+$ cells were present in all apico-basal regions of the IZ, SP and CP (**J**–**L**, from boxed regions in **G**–**I**). Furthermore, many of these cells were also $4A4^+$ (**M**–**R**, taken from boxed regions in **J**–**L**). A minority of $H3^+/4A4^+$ cells in the IZ (**N**, **R**, *double arrowhead*), SP (**P**, *double arrowhead*) possessed short processes that extended a short distance toward the pia. Scale bars: **A**–**I** 200 μm, **G**–**I** 100 μm, **J**–**L** 50 μm, *a′*–*f′*, **M**–**R** 25 μm

of the T-box family labels C–R, layer VI and subplate cells (Bulfone et al. 1995; Hevner et al. 2001). At E13, Tbr1-immunopositive cells in the PP did not express 4A4 despite the presence of $4A4^+$ cells in this compartment (Suppl. Fig. 1G–I). Calretinin is a neuron-specific calcium-binding protein that is used as a marker of Cajal-Retzius cells (Meyer et al. 1998) and is also expressed in a subpopulation of interneurons (reviewed in DeFelipe 1993). Similar to TUJ1, PP cells with occasional VZ-directed processes were visualized by calretinin (Suppl. Fig 1J–M) and calbindin (not shown; Meyer et al. 1998), another calcium-binding protein which labels a population of interneurons and layer V pyramidal neurons (Hevner et al. 2003). No colocalisation of H3 was observed in either calretinin- or calbindin-expressing cells in E13 rat preplate. At E14, Reelin expression which is observed in C-R cells (Meyer and Wahle 1999) was not observed in $H3^+$ cells in the PP (Suppl. Fig. 1N–P).

Later developmental stages were also examined to determine whether EVPCs expressed markers indicative of a prior commitment to a cell type-specific lineage. Tbr1 was expressed in cells of the CP and SP (Suppl. Fig. 2A–C), and was not found in 4A4-expressing EVPCs. Calbindin immunoreactivity was mainly localized to the MZ and lower portion of the CP, in addition to migratory cells, identifiable by their processes (Suppl. Fig. 2D,E), and $4A4^+$ EVPCs were calbindin-immunonegative (Suppl. Fig 2F) at E17.5. At the same age, $Reelin^+$ cells were confined to the

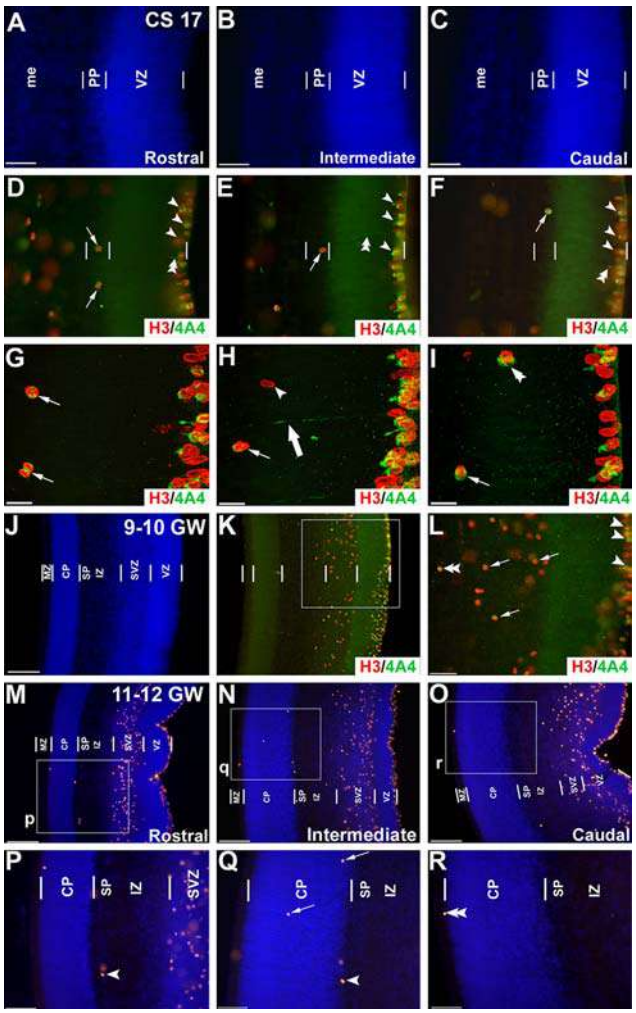


Fig. 6 Extra-ventricular proliferating cells in human preplate stage cortex express phosphorylated vimentin and persist in early fetal cortex. Double-exposure images of rostral (**A**), intermediate (**B**) and caudal (**C**) coronal sections of a Stage 17 (CS 17; E40–41) human brain labelled with H3 (*red*) and 4A4 (*green*). The majority of $H3^+$ cells at the ventricular surface also expressed 4A4 (*arrowheads*). A minority of $4A4^+$ cells have pial-directed processes (**A**–**C**, *double arrowheads*, and see **H** for pial-directed process, indicated by a *thick arrow* from a radial glia in the VZ). In addition, extra-ventricular mitoses, revealed by H3/4A4 were present in the PP (**A**–**C**, *arrows*). Co-expression of H3 and 4A4 in these cells was confirmed by confocal microscopy (**G**–**I**, *arrows*), although some $H3^+$ cells that were 4A4-immunonegative were observed (**H**, *arrowhead*). Occasional double-positive cells were present in the basal VZ (**I**, *double arrowheads*). **G** At 9–10 gestational weeks (GW), the germinal zone consisted of the VZ/SVZ, and the IZ, SP, CP and MZ were also present in the developing cortical wall as revealed by bisbenzimide (blue) counterstaining. **J** H3- and 4A4-immunoreactivity was primarily restricted to the VZ/SVZ (**K**, **L**, *arrowheads*, *arrows*) although double-positive cells were present in the apical portion of the IZ (**K**, *double arrowheads*). **M**–**O** Later during the early fetal period at 11–12 GW, $H3^+$ cells were more prominent in extraventicular compartments (**M**–**R**). Such EVPCs were observed in the IZ/SP (**P**, **Q**, *arrowhead*), in the lower and middle CP (**Q**, *arrows*) and at the CP–MZ interface (**Q**) and in the MZ (**R**, *double arrowhead*). Scale bars: **M**–**O** 200 μm, **P**–**R** 100 μm, **A**–**F**, **J**–**L** 50 μm, **G**–**I** 20 μm

MZ and did not share expression with $H3^+$ cells located external to the germinal zones (Suppl. Fig. 2G–I).

In addition to using a panel of markers that label early populations of cell types that may be generated locally in the pallium, we wished to rule out the possibility interneurons which migrated from the subpallium (reviewed Parnavelas 2000; Corbin et al. 2001; Marin et al. 2001) may account for EVPCs in the developing cortical wall. The anti-Dll antibody was used as a pan-Dlx marker (Kohtz et al. 2001) to label interneurons derived from the ventral telencephalon. During the preplate stage, Dll-immunopositive (Dll^+) cells were restricted to the progenitor and mantle regions of the ganglionic eminences (not shown) and so could not account for $4A4^+$ cells in the PP of the pallium. Later, at E16.5, streams of Dll^+ cells were observed in the MZ and the SVZ/lower IZ in accordance with known migratory patterns of tangentially migrating interneurons. No colocalisation of 4A4 was observed in Dll^+ cells in the pallium (Suppl. Fig. 2L) and this was also the case for GABA, another marker of interneurons at E13 and E17.5 (not shown).

Another cell type thought to be of ventral telencephalic origin is oligodendrocytes (Perez Villegas et al. 1999; Nery et al. 2001), and such ventral telencephalic sources have recently been identified (Kessaris et al. 2006). Immunohistochemistry for the oligodendrocyte marker, NG2, predominantly labelled the developing vasculature in the ventral telencephalon, and to a lesser extent in the pallium at E13 (Suppl. Fig 2M,N). $H3^+$ cells were located proximal to NG2-immunopositive ($NG2^+$) blood vessels although as aforementioned, cells closely associated with vasculature were excluded from the quantitative analysis. At E13.5 (Suppl. Fig. 2M–O) and E17.5 (not shown) no coexpression of NG2 and H3 was observed

In addition, to exclude the possibility that $H3^+$ or $H3^+/4A4^+$ cells in extra-ventricular compartments were post-mitotic cells that still expressed M phase-specific markers, we visualized $H3^+/4A4^+$ cells with the To-Pro 3 iodide nuclear stain for confocal microscopy. In many $H3^+/4A4^+$ cells in extra-ventricular compartments the cleavage furrow and nascent daughter cells were clearly visible (not shown). Double immunohistochemistry for calretinin/4A4 and calbindin/4A4 in human cortex at 11–12 GW did not reveal any double-positive cells in the developing cortical wall (not shown). However, due to scarcity of material we were not able to complete comparative analysis of these markers in human tissue.

Extraventricular-proliferating cells do not express Tis21 indicating imminent mitotic cell divisions are non-neurogenic and a subset are proliferating microglia

Subsequently, H3 immunolabelling was performed in sections from Tis21-GFP mice at E12.5 and E15.5. The

Tis21 gene identifies neuroepithelial cells that will generate neurons at their next division (Iacopetti et al. 1999). At E12.5, Tis21-GFP expression predominantly occurred in the basal portion of the VZ (Haubensak et al. 2004), and we did not observe Tis21-GFP expression in $H3^+$ cells in the PP at E12.5 (not shown). At E15.5, strong Tis21-GFP expression was observed in the GZ and H3 immunolabelling was predominant in the GZ (Fig. 7B, E and C, F, respectively). High power confocal microscopy images of the cortical wall show that Tis21-GFP was preferentially expressed by precursors located in the basal portion of the VZ although some Tis21-GFP^+ cells were located in the IZ (Fig. 7H–I) in agreement with the spatio-temporal profile of Tis21-GFP expression as previously described (Haubensak et al. 2004). As documented in rat cortex, $H3^+$ cells were located in the VZ, SVZ, IZ and CP (Fig. 7G–I). Tis21-GFP expression was not observed in $H3^+$ cells in the IZ (Fig. 7I, i′), indicating that these cells were either not neurogenic in their final division, or not in their final division. Tis21-GFP expression was not observed in the SP, CP or MZ at E15.5.

Last, we used the lectin RCA-1 as a marker of microglia (Suzuki et al. 1988; Maslinska et al. 1998; Bystron et al. 2002). In E13 rat cortex, no RCA-1-immunoreactive ($RCA\text{-}1^+$) cells were observed, although developing brain vasculature was labelled (Wu et al. 1993), confirming that EVPCs in the preplate did not correspond to microglia (not shown). Double immunofluorescence for RCA-1 and H3 at E19, showed few double-positive cells, many of which appeared in the GZ and to a lesser extent in the IZ, SP and CP (not shown). Nonetheless, the colonisation of rat cortex by microglia has been previously described and primarily occurs during the postnatal period (Dalmau et al. 2003). Therefore, proliferating microglia in the rodent cortex may only constitute a minority of $H3^+$ EVPCs at the end of corticogenesis. In human cortex, however, we show that microglia, many of which are proliferating, are present in the cortical wall at a much earlier comparative stage of development than in rodent. In CS 20 human cortex, both $H3^+$ and H3-immunonegative $RCA\text{-}1^+$ cells were observed in both the VZ and the PP (Fig. 7J). $RCA\text{-}1^+$ cells with and devoid of processes were observed, perhaps indicating different stages of differentiation.

Discussion

The primate neocortex is 100-fold larger and is generated during a 10-fold longer corticogenetic period than in rodent (Rakic 1974). A number of studies have demonstrated marked neuroanatomical differences in cortical development between primate and rodent species (Meyer et al. 2000; Letinic et al. 2002; Smart et al. 2002; Altman and Bayer 2002; Lukaszewicz et al. 2005; Bystron et al. 2005a, 2006). Such comparative neuroanatomical and evolutionary data highlight the importance of examining primate, and wherever possible human tissue, to gain insight into which aspects of cortical development are conserved or diverge between rodent and primate.

In this study we have compared the patterns of 'extraventricular proliferating cells' (EVPCs) in rat and human cortex. We found that: (1) the extent of extra-ventricular mitoses in the PP is similar in rat and human cortex; (2) later in development EVPCs occur in the IZ, SP and CP, but not the MZ in rat. Similarly in human cortex EVPCs occurred in the IZ (including subplate), CP and, in contrast to rat, the MZ; (3) the majority of EVPCs in rat and human PP were immunoreactive to phosphorylated vimentin; (4) EVPCs in rat cortex did not express neuronal markers, or exhibit Tis21-GFP expression. A subset of EVPCs in during late corticogenesis in rat, but at preplate stage in human was identified as proliferating microglia. We discuss these results in relation to known timetables of cell generation and the appearance of specific cell types in the rodent and human pallium.

The temporal appearance and gradients of preplate mitoses in rat and human cortex suggests a likely role in seeding the subventricular zone

Valverde et al. (1995) described mitotic figures present in the rat PP at E12 and E13, and estimated that these represented ~2.5% of the mitoses in the VZ. Here, using H3 immunohistochemistry, we found that the occurrence of PP mitoses is higher than previously estimated, representing ~7.55% of the $H3^+$ cells in the VZ. Quantitative analysis of preplate mitoses revealed both rostro-caudal and ventro-medial gradients at E13, which is consistent with known histogenetic gradients, so the appearance of PP mitoses reflects that of their VZ counterparts. Previous studies in human cortex have described rare mitoses in the preplate (Zecevic 2004) and the basal part of the early cortical primordium (Bystron et al. 2006). However, our quantitative analysis estimates that PP mitoses are more predominant and representing ~6.19% of $H3^+$ cell density in the VZ in CS 16–20 human cortex. As in rodent, H3 cell density in the PP was more prominent in lateral compared to medial cortex, but whereas a rostro-caudal gradient was observed in lateral cortex, intermediate cortical regions medially exhibited the highest density of $H3^+$ cells. Although histogenetic gradients in human occur along the lateral-medial axis as in rodent, along the rostro-caudal axis, medial regions are more advanced (Zecevic 1993), as observed in medial cortex in the present study.

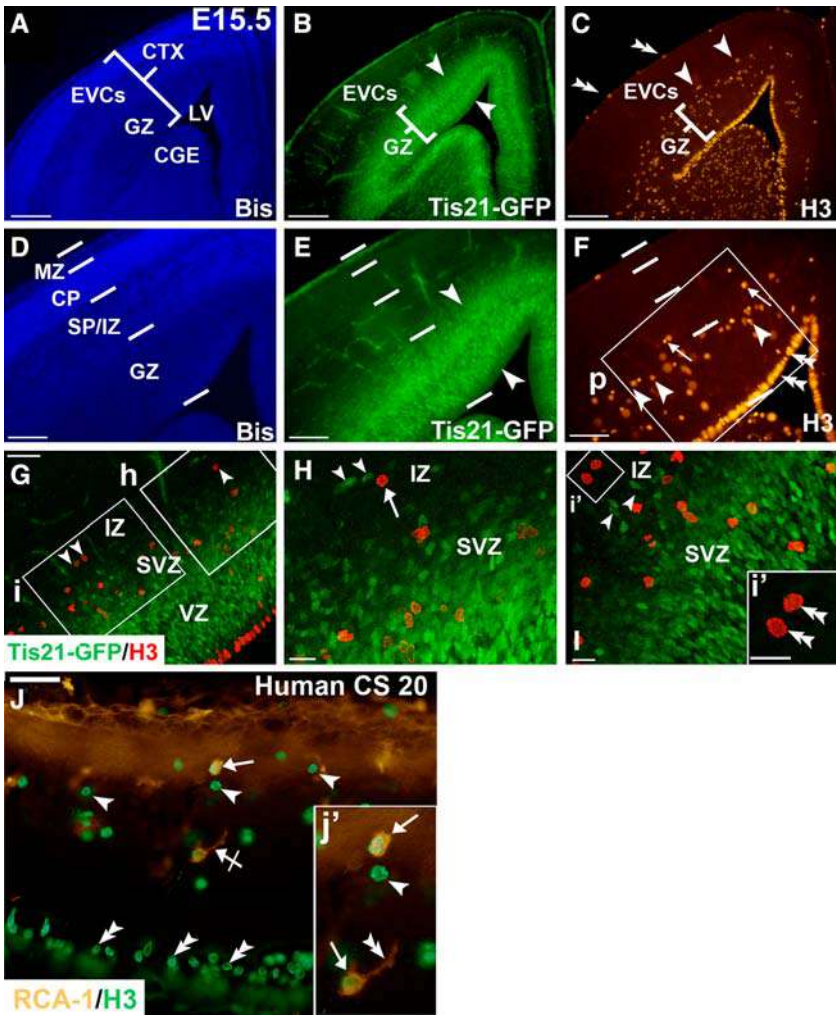


Fig. 7 Non-neurogenic divisions and proliferating microglia are observed in extra-ventricular compartments in the cortical wall (**A**–**I**) Immunolabelling for H3 (*red*) in E15.5 sections from Tis21-GFP mice. **A** Bisbenzimide (*blue*) counterstaining demonstrated the germinal zone (GZ) and extraventricular compartments (EVCs) of the cortical wall. **B** Tis21-GFP fluorescence (*green*) occurred in the GZ (*arrowheads*), whereas **C** $H3^+$ cells occurred not only in the GZ, but also in the EVCs (*arrowheads*) and in the pia (*double arrowheads*). **D**–**F** High power views of **A**–**C**. **E** As in **B**, Tis21-GFP-positive (Tis21-GFP^+) cells occurred in the GZ (*arrowheads*). **F** The majority of the $H3^+$ cells were located at the apically in the VZ (*double arrowheads*) but also occurred in the SVZ (*arrowheads*) and in the IZ (*arrows*). **G**–**I** GFP fluorescence was most intense in the basal portion of the ventricular zone (VZ), as apposed to the apical VZ where $H3^+$ cells occurred, in addition to the SVZ and a few cells located in the IZ (*arrowheads*). **H** Some Tis21-GFP^+ cells were also located in the IZ (*arrowheads*), in addition to H3 immunoreactivity (*arrow*), from boxed region in **G**. **I** Tis21-GFP^+ cells (*arrowheads*) and $H3^+$ cells (boxed in *i′*) in the IZ from boxed region in **G**. The $H3^+$ cells in the IZ (*i′*, *double arrowheads*) did not show Tis21-GFP expression. **J** Immunoreactivity to H3 (*green*) and the lectin *Riccinis communis agglutinis* (RCA-1; *red*) in CS 20 human cortex (E47–49). As in rodent, $H3^+$ cells were located at the apical surface of the VZ (*double arrowheads*) and in the upper VZ and lower PP (*arrowheads*), which did not express RCA-1. A minority of $H3^+$ cells in the PP (*arrow*) and middle VZ (*crossed arrow*) were likely to be microglia as indicated by RCA-1 immunoreactivity. (*j′*) A $H3^+$/RCA-1-immuno-negative, and a double-labelled cell in the PP (*arrow*) from boxed region in **J**. The double-positive cell in the middle VZ (*lower arrow*) also displayed a short process (*double arrowhead*). Abbreviations: *CGE* caudal ganglionic eminence, *CTX* cortex; **A**–**F**, **J** epifluorescence microscopy; **G**–**I**, *i′*: confocal microscopy. Scale bars: **D**–**F**, **G** 100 μm; **A**–**C**, **J** 50 μm; **H**, **I**, *i′* 20 μm

Previous descriptions of mitotic figures in the PP have been implicated as a possible neuronal progenitor population which may produce C-R cells in rat (Valverde et al. 1995) and human (Zecevic et al. 1998), a putative SVZ that may contribute to neurogenesis as early as E13 in the mouse (Hinds and Ruffett 1971; Smart 1985) and a nascent SVZ in human (Zecevic 2004). However, sources of Cajal-Retzius cells at the cortical hem, cortico-striatal border and septum (Bielle et al. 2005) described in rodent, would seemingly discount the possibility that PP divisions would generate Cajal-Retzius cells. Valverde and colleagues (1995) postulated that PP mitoses could arise by a

number of interkinetically migrating cells in the basal portion of the VZ, becoming 'displaced' into the PP, forming the SVZ. Indeed, a ^{3}H-TdR pulse followed by a short survival time revealed heavily labelled PP cells, which due to known cell cycle times in the VZ (Nowakowski et al. 1989; Takahashi et al. 1993), must have derived from local proliferating cells in the PP (Valverde et al. 1995). Therefore, short-term BrdU labelling (Valverde et al. 1995) and mitotic marker analysis (present study) suggest that cells undergo both S- and M-phases of the cell cycle in the PP. Furthermore, the timing of PP mitoses and appearance and their developmental gradients as determined from our data suggest the timing could indeed implicate PP mitoses as the forerunner of the putative SVZ. Indeed, further support for this hypothesis may be evidenced in the present study by the lack of Tis21-GFP expression in $H3^{+}$ cells of the PP at E12.5, meaning that these cells may not imminently undergo neuron-generation divisions. Tbr2 expression in rodent cortex labels intermediate progenitors and post-mitotic cells (Englund et al. 2005). Recently, $Tbr2^{+}/BrdU^{+}$ cells in mouse preplate at E12.5 have been described (Quinn et al. 2006), again suggesting intermediate progenitor cells (i.e. the SVZ) may originate in the preplate. Interestingly, in the turtle dorsal cortex which does not have an SVZ, few abventricular (non-surface) mitoses occur (Martinez-Cerdeño et al. 2006). Certainly how the cellular structure of the SVZ appears during early corticogenesis has not yet been elucidated, although classic histological studies in rodent suggested that cells of the VZ set up the SVZ (Smart and McSherry 1982). Recent data obtained from $Pax6^{+/+} \leftrightarrow Pax6^{-/-}$ chimeras describes a reduction in co-labelled $Tbr2^{+}/BrdU^{+}$ cells in the preplate, in addition to few IPCs that co-express H3 and Tbr2 in the $Pax6^{-/-}$ telencephalon at E12.5 (Quinn et al. 2006). These findings seemingly provide indirect evidence of a role of the VZ in establishing an abventricular Tbr2 proliferative population.

Prior immunohistochemical analyses in early human cortex also lend credence that PP mitoses may represent the putative SVZ. Mitoses in the basal portion of the cortical primordium are present as early as CS13 (Bystron et al. 2006) and more abundantly at CS16–20 (this study). Tbr2 is barely detectable at 4–5 GW (Bystron et al. 2005b), but is observed in the human preplate at 6–7 GW (Bystron et al. 2005b), coinciding with the previously described appearance of the SVZ in human at 7 GW (Mollgard and Schumacher 1993; Zecevic 1993). However, further defining the Tbr2 cells described in the human PP at 6–7 GW is important as Tbr1 expression was also observed in this compartment (Bystron et al. 2005b). Thus, co-expression studies showing the colocalisation or absence of post-mitotic markers, e.g. TUJ1, in Tbr2 cells in the human PP would be very informative.

However, further understanding of cortical neuron generation in human is complicated not only by a limitation of technical approaches but by the complexities of corticogenesis. Cortical neurons are predominantly generated a primate-specific anatomical compartment called the 'Outer Subventricular Zone' (OSVZ) in macaque (Smart et al. 2002; Lukaszewicz, et al. 2005) which is also present in human cortex (Zecevic et al. 2005). It is conceivable that EVPCs in the macaque PP may contribute to formation of the early 'Inner Subventricular Zone' (which resembles the rodent SVZ) and that this compartment later generates the OSVZ.

Phosphorylated vimentin, 4A4, expression in extra-ventricular proliferating cells

We next considered further the possibility that EPVCs represent displaced RG that remain proliferative in compartments external to the ventricular zone, by performing double-labelling analysis for H3 and phosphorylated vimentin, 4A4, previously described as a marker of mitotic radial glia (Kamei et al. 1998; Götz et al. 2002). However, although 4A4 clearly cells that are RG in the rodent VZ and human VZ (Weissman et al. 2003), we concluded that the association of the mitotic marker 4A4 with the cell type radial glia is misleading. Firstly, we found that 4A4 expression was also observed in cells associated with vasculature and outside of the developing telencephalon and so do not correspond to RG. Secondly, it is important not to confound the morphological definition RG as cells in VZ/SVZ with ascending pial-directed processes (Rakic 1972) with precursor cells with neurogenic potential. $4A4^{+}$ cells in the IZ in rodent (Kamei et al. 1998) and IZ and SGL of human cortex (Howard et al. 2006) have been described as radial glia. Occasional 4A4/Tbr2 colocalisation and Pax6 expression (Englund et al. 2005) in cells equivalent to EPVCs indicate that these cells may be capable of generating neurons. However, definitive estimations of neurogenic potential based on immunohistochemical analysis is hampered by the fact that Tbr2 expression is observed in post-mitotic cells as well as intermediate progenitor cells (Englund et al. 2005). To this end, we examined H3 expression in Tis21-GFP mice as an alternative method to determine whether EVPCs may produce neurons. At E15.5 we did not observe colocalization of H3 in Tis21-GFP^{+} cells in the IZ, although a systematic developmental study was not undertaken. This is somewhat surprising as the Tis21-GFP^{+} IZ cells (see Fig. 7G–I) correspond to the SPP described by Takahashi and colleagues (1995) which is assumed to be a spill-over of SVZ cells into the IZ region. Nonetheless, the lack of Tis21-GFP expression in IZ EVPCs does not definitively rule out that EVPCS are neuronal precursors as: (1) Tis21

expression specifically labels neuronal precursors on their terminal division; (2) Tis21-GFP expression peaks during the G1-S phase transition and (3) Tis21-GFP expression is observed in some newborn neurons outside of the GZ by passive inheritance (Haubensak et al. 2004). Alternative methods to provide conclusive evidence that EVPCs have the potential to generate cortical neurons are not easily demonstrable. First, the retroviral infection methods used to track cortical progenitors (Noctor et al. 2004) would preclude selective visualisation of progenitors in the PP. Second, backlabelling EVPCs in the PP using pial application of carbocyanine dyes or fluorescently tagged microspheres, as used previously for RG (Noctor et al. 2002; Weissman et al. 2003), is not an option as 4A4 immunolabelling indicated that the vast majority of these cells are devoid of pial-directed processes or only have short processes. However, the Nex-positive cell lineage, which demarks neuronal phenotype expression, has shown that Nex-positive cells from the IZ and CP were capable of neuron production upon transplantation into wildtype hosts (Wu et al. 2003). However, to what extent this occurs *in vivo* remains to be elucidated.

4A4 antibody staining labels only a proportion of pial-directed processes, as detection of numerous $4A4^+$ pial-directed processes is hampered due to thinning of the RG process during mitosis (Miyata et al. 2001; Weissman et al. 2003). Previously, Howard and colleagues (2006) described $4A4^+$ progenitors in human cortex at 4–5 GW that were devoid of pial-directed processes and concluded that this was a phase of symmetrical division and progenitor pool enlargement. However, we found pial-directed processes in $4A4^+$ VZ cells at CS 17 (see Fig. 6H). This is likely a technical difference but our data suggests that symmetrical division may not be exclusive in human at 4–5 GW as previously considered (Howard et al. 2006), as the radial glial guide for newly born neurons from asymmetric divisions is present. Also in human cortex, Howard and colleagues (2006) state that occasional $4A4^+$ cells in the IZ and subpial granular layer had processes oriented apically toward the ventricular surface, which may serve as a guide for migratory interneurons. In the current study, processes emanating from $4A4^+$ cells were only observed in the IZ and SP of rat cortex at E19, and the processes were all directed towards the pia. $4A4^+$ processes were not observed in our early human fetal specimens. Therefore, our data do not indicate EVPCs may serve as a guide for migratory interneurons. However, the possibility that interneurons can be locally generated in the human pallium (Letinic et al. 2002) may correlate with the hypothetical migratory scaffold for interneurons proposed (Howard et al. 2006). This further highlights the potential complexity in applying known developmental mechanisms to human relevance.

Extra-ventricular proliferating cells do not express early post-mitotic markers indicating prior commitment to neuronal, interneuronal or an oligodendrocyte lineage, and are Tis21-GFP-negative

Subsequently, we sought to determine whether EVPCs express mitotic and post-mitotic markers concomitantly. Seemingly contradictory, this scenario is conceivable in the event that post-mitotic cells re-enter the cell cycle in extra-ventricular locations. The expression of post-mitotic markers reflects neuronal commitment, and this specification is thought to occur around the time of terminal mitosis in the dorsal telencephalic germinal zone (McConnell 1988). Similarly, cells undergoing tangential migration to the dorsal telencephalon from ventral sources are only rarely mitotically active (Anderson et al. 2001; Nery et al. 2003). However, recently it has been shown that proliferating $Pax6^+$ and $Dlx2^+$ cells exist along the embryonic lateral cortical stream migratory route to basal telencephalic structures (Carney et al. 2006). Early post-mitotic neurons in the PP expressed pan-neuronal or cell type-specific markers such as TUJ1, Tbr1, calretinin, calbindin and Reelin in patterns consistent with prior studies in which they were initially described (see Menezes and Luskin 1994; Bulfone et al. 1995; Meyer et al. 1998; Meyer and Wahle 1999; Hevner et al. 2001). However, EVPCs in early and late rat cortex did not express post-mitotic neuronal markers of dorsal or ventral telencephalic origin. Prior studies in human cortex showed that post-mitotic neurons in the human PP were not immunoreactive to a panel of ventral telencephalic markers (Dlx2, Dll, Nkx2.1) suggesting that these cells were locally generated in the pallium (Rakic and Zecevic 2003, Bystron et al. 2006). Moreover, initiation of GABA immunoreactivity is first detected in the lateral wall of the pallium at 6.5 GW, CS 19–20 (Zecevic and Milosevic 1997), as apposed to earlier developmental stages where EVPCs in the human PP are first observed. Taken together, it seems likely that $H3^+$ cells in the human PP are a local precursor population in the pallium.

Extra-ventricular proliferating cells at mid-late stages of corticogenesis may represent microglia and glial precursors

RCA-1 expression is an early marker of microglia in the human telencephalon (Andjelkovic et al. 1998; Rezaie et al. 2005). Lectin-positive microglia have been described in the MZ (PP of this study) at 5.5 GW in human (Andjelkovic et al. 1998) and RCA-1-positive microglia occurred in the VZ and MZ (PP, current study) of human cortex at 5–7 GW (Zecevic et al. 1998). Recently, Iba1-positive microglia in the plexiform layer of the cortical

anlagen, prior to cortical plate formation have been described (Monier et al. 2006). We show that proliferating microglia are present in the rat cortical wall from late stages of gestation, and in contrast are present much earlier in development in human, in the VZ and PP, Thus, in rat cortex EVPCs are not likely to represent microglia to a significant extent as microglia development mainly occurs postnatally with 92–99% of microglia immunoreactive to Proliferating Cell Nuclear Antigen (PCNA) at P9 (Dalmau et al. 2003). Indeed, EVPCs during the terminal phase of corticogenesis in rat may generate glia, as shown by short term BrdU labelling (Levers et al 2001). A few mitotic figures in the IZ of human striate cortex at 8–9 and 13–15 GW has also been described (Masood et al. 1990). Rare PCNA-immunopositive cells were observed in the IZ (including the developing SP) of human cortex at 12–15 GW, and in the IZ and SP later in development at 22–24 GW (Simonati et al. 1999) and in the CP (Tiu 2001). Gliogenesis in human is known to commence and peak at 15–25 GW where proliferating cells in the IZ have been identified by anti-PCNA immunostaining, and some of these cells expressed GFAP (Kendler and Golden 1996). Therefore, we may infer that the EVPCs observed in early human fetal cortex do not occur during the appropriate temporal time frame considered for gliogenesis. On the other hand, as proliferating microglia are present much earlier in development in human than in rodent, some EVPCs may generate microglia locally in the pallium.

Concluding remarks

Previous studies have described the enhanced complexity in primate of several embryonic anatomical compartments that orchestrate the generation of the cerebral cortex, such as preplate formation (Meyer et al. 2000), the intermediate zone (Altman and Bayer 2002) the subplate (Kostovic and Rakic 1990; Smart et al. 2002) and the early cortical primordium (Bystron et al. 2006). Cell cycle analysis revealing the important role of the primate OSVZ (Smart et al. 2002; Lukaszewicz et al. 2005) and suggested variation in cell cycle length (Kornack and Rakic 1998) already indicated mechanistic differences in corticogenesis exist between the rodent and primate cortex. Taken together, these studies highlight the importance of examining aspects of brain development in primate specimens. Interestingly, the current study provides evidence that the early appearance of EVPCs in the preplate are shared in the rodent and human brain.

Acknowledgments This work was supported by Grants from The European Community (QLRT-1999-30158), The Wellcome Trust (063974/B/01/Z), Human Frontier Science Program (RGP0107/2001), Medical Research Council and RGBI 01-04-48819. RSEC was supported by a MRC studentship and Mary Goodger Scholarship (Oxford Medical Science Division). We are grateful to Dr. Henry Kennedy, Dr. Colette Dehay, Dr. Wieland Huttner, Dr. Alessio Attardo and Dr. Joshua Corbin for their thoughtful comments on a previous version of this manuscript and Prof. Colin Blakemore for valuable discussions regarding this study. The authors would also like to thank Drs. Huttner and Attardo for providing the Tis21-GFP brains used in this study. Dr. Ole Paulsen kindly provided advice on quantitative analysis.

References

Altman J, Bayer SA (2002) Regional differences in the stratified transitional field and the honeycomb matrix of the developing human cerebral cortex. J Neurocytol 31:613–632

Anderson SA, Marin O, Horn C, Jennings K, Rubenstein JL (2001) Distinct cortical migrations from the medial and lateral ganglionic eminences. Development 128:353–363

Andjelkovic AV, Nikolic B, Pachter JS, Zecevic N (1998) Macrophages/microglial cells in human central nervous system during development: an immunohistochemical study. Brain Res 814:13–25

Angevine J, Sidman RL (1961) Autoradiographic study of cell migration during histogenesis of cerebral cortex in the mouse. Nature 192:766–768

Bayer SA, Altman J (1991) Neocortical development

Berry M, Rogers AW (1965) The migration of neuroblasts in the developing cerebral cortex. J Anat 99:691–709

Bielle F, Griveau A, Narboux-Neme N, Vigneau S, Sigrist M, Arber S, Wassef M, Pierani A (2005) Multiple origins of Cajal-Retzius cells at the borders of the developing pallium. Nat Neurosci 8:1002–1012

Boulder Committee (1970) Embryonic vertebrate central nervous system: revised terminology. Anat Rec 166:257–262

Bulfone A, Smiga SM, Shimamura K, Peterson A, Puelles L, Rubenstein JL (1995) T-brain-1: a homolog of Brachyury whose expression defines molecularly distinct domains within the cerebral cortex. Neuron 15:63–78

Bystron IP, Smirnov EB, Otellin VA, Wierzba-Bobrowicz T, Dymecki J. (2002) Suspensional reaggregates of human foetal neocortex and tegmentum as objects of neurotransplantation. Folia Neuropathol 40(2):75–85

Bystron I, Molnár Z, Otellin V, Blakemore C (2005a) Tangential networks of precocious neurons and early axonal outgrowth in the embryonic human forebrain. J Neurosci 25:2781–2792

Bystron I, Hevner RF, Blakemore C (2005b) The columnar organization of the neuroepithelium in human cortical primordium. Soc Neurosci Abstr P.144.3

Bystron I, Rakic P, Molnar Z, Blakemore C (2006) The first neurons of the human cerebral cortex. Nat Neurosci 9:880–886

Carney RSE, Alfonso B, Cohen D, Dai H, Nery S, Stoica B, Slotkin J, Bregman BS, Fishell G, Corbin JG (2006) Cell migration along the lateral cortical stream to developing basal telencephalic limbic structures. J Neurosci 26:11562–11574

Corbin JG, Nery S, Fishell G (2001) Telencephalic cells take a tangent: non-radial migration in the mammalian forebrain. Nat Neurosci 4(Suppl):1177–1182

Dalmau I, Vela JM, Gonzalez B, Finsen B, Castellano B (2003) Dynamics of microglia in the developing rat brain. J Comp Neurol 458:144–157

DeFelipe J (1993) Neocortical neuronal diversity: chemical heterogeneity revealed by colocalisation studies of classic

neurotransmitters, neuropeptides, calcium-binding proteins, and cell surface molecules. Cereb Cortex 3:273–289

Englund C, Fink A, Lau C, Pham D, Daza RA, Bulfone A, Kowalczyk T, Hevner RF (2005) Pax6, Tbr2, and Tbr1 are expressed sequentially by radial glia, intermediate progenitor cells, and postmitotic neurons in developing neocortex. J Neurosci 25:247–251

Estivill-Torrus G, Pearson H, van Heyningen V, Price DJ, Rashbass P (2002) Pax6 is required to regulate the cell cycle and the rate of progression from symmetrical to asymmetrical division in mammalian cortical progenitors. Development 129:455–466

Gal JS, Morozov YM, Ayoub AE, Chatterjee M, Rakic P, Haydar TF (2006) Molecular and morphological heterogeneity of neural precursors in the mouse neocortical proliferative zones. J Neurosci. 26(3):1045–1056

Götz M, Hartfuss E, Malatesta P (2002) Radial glial cells as neuronal precursors: a new perspective on the correlation of morphology and lineage restriction in the developing cerebral cortex of mice. Brain Res Bull 57:777–788

Haubensak W, Attardo A, Denk W, Huttner WB (2004) Neurons arise in the basal neuroepithelium of the early mammalian telencephalon: a major site of neurogenesis. Proc Natl Acad Sci USA 101:3196–3201

Hevner RF, Neogi T, Englund C, Daza RA, Fink A (2003) Cajal-Retzius cells in the mouse: transcription factors, neurotransmitters, and birthdays suggest a pallial origin. Brain Res Dev Brain Res 141:39–53

Hevner RF, Shi L, Justice N, Hsueh Y, Sheng M, Smiga S, Bulfone A, Goffinet AM, Campagnoni AT, Rubenstein JL (2001) Tbr1 regulates differentiation of the preplate and layer 6. Neuron 29:353–366

Hevner RF, Hodge RD, Daza RA, Englund C. (2006) Transcription factors in glutamatergic neurogenesis: conserved programs in neocortex, cerebellum, and adult hippocampus. Neurosci Res 55(3):223–233

Hinds JW, Ruffett TL (1971) Cell proliferation in the neural tube: an electron microscopic and golgi analysis in the mouse cerebral vesicle. Z Zellforsch Mikrosk Anat 115:226–264

Howard B, Chen Y, Zecevic N (2006) Cortical progenitor cells in the developing human telencephalon. Glia 53:57–66

Iacopetti P, Michelini M, Stuckmann I, Oback B, Aaku-Saraste E, Huttner WB (1999) Expression of the antiproliferative gene TIS21 at the onset of neurogenesis identifies single neuroepithelial cells that switch from proliferative to neuron-generating division. Proc Natl Acad Sci USA 96:4639–4644

Jones L, López-Bendito G, Gruss P, Stoykova A, Molnár Z (2002) Pax6 is required for the normal development of the forebrain axonal connections. Development 129:5041–5052

López-Bendito G, Sturgess K, Erdelyi F, Szabo G, Molnár Z, Paulsen O (2004) Preferential origin and layer destination of GAD65-GFP cortical interneurons. Cerebral Cortex 14(10): 1122–1133

Kamei Y, Inagaki N, Nishizawa M, Tsutsumi O, Taketani Y, Inagaki M (1998) Visualization of mitotic radial glial lineage cells in the developing rat brain by Cdc2 kinase-phosphorylated vimentin. Glia 23:191–199

Kendler A, Golden JA (1996) Progenitor cell proliferation outside the ventricular and subventricular zones during human brain development. J Neuropathol Exp Neurol 55:1253–1258

Kessaris N., Fogarty M., Iannarelli P., Grist W., Wegner M, Richardson W.D. (2006) Competing waves of oligodendrocytes in the forebrain and postnatal elimination of an embryonic lineage. Nat Neurosci 9:173–179

Kohtz JD, Lee HY, Gaiano N, Segal J, Ng E, Larson T, Baker DP, Garber EA, Williams KP, Fishell G (2001) N-terminal fatty-acylation of sonic hedgehog enhances the induction of rodent ventral forebrain neurons. Development 128:2351–2363

Kornack DR, Rakic P (1998) Changes in cell-cycle kinetics during the development and evolution of primate neocortex. Proc Natl Acad Sci USA 95:1242–1246

Kostovic I, Rakic P (1990) Developmental history of the transient subplate zone in the visual and somatosensory cortex of the macaque monkey and human brain. J Comp Neurol 297:441–470

Lee MK, Rebhun LI, Frankfurter A (1990) Posttranslational modification of class III beta-tubulin. Proc Natl Acad Sci USA 87:7195–7199

Letinic K, Zoncu R, Rakic P (2002) Origin of GABAergic neurons in the human neocortex. Nature 417:645–649

Levers TE, Edgar JM, Price DJ (2001) The fates of cells generated at the end of neurogenesis in developing mouse cortex. J Neurobiol 48:265–277

Lukaszewicz A, Savatier P, Cortay V, Giroud P, Huissoud C, Berland M, Kennedy H, Dehay C (2005b) G1 phase regulation, area-specific cell cycle control, and cytoarchitectonics in the primate cortex. Neuron 47:353–364

Luskin MB, Shatz CJ (1985) Studies of the earliest generated cells of the cat's visual cortex: cogeneration of subplate and marginal zones. J Neurosci 5:1062–1075

Malatesta P, Hartfuss E, Gotz M (2000) Isolation of radial glial cells by fluorescent-activated cell sorting reveals a neuronal lineage. Development 127:5253–5263

Marin-Padilla M (1971) Early prenatal ontogenesis of the cerebral cortex (neocortex) of the cat (Felis domestica). A Golgi study. I. The primordial neocortical organization. Z Anat Entwicklungsgesch 134:117–145

Marin-Padilla M (1972) Prenatal ontogenetic history of the principal neurons of the neocortex of the cat (Felis domestica). A Golgi study. II. Developmental differences and their significances. Z Anat Entwicklungsgesch 136:125–142

Marin O, Rubenstein JL (2001) A long, remarkable journey: tangential migration in the telencephalon. Nat Rev Neurosci 2:780–790

Martinez-Cerdeno V, Noctor SC, Kriegstein AR (2006) The role of intermediate progenitor cells in the evolutionary expansion of the cerebral cortex. Cereb Cortex 16(Suppl 1):i152–161

Maslinska D, Laure-Kamionowska M, Kaliszek A (1998) Morphological forms and localization of microglial cells in the developing human cerebellum. Folia Neuropathol 36:145–151

Masood F, Wadhwa S, Bijlani V (1990) Early development of visual cortex in human fetuses. Arch Ital Anat Embriol 95:1–10

McConnell SK (1988) Development and decision-making in the mammalian cerebral cortex. Brain Res 472:1–23

Menezes JR, Luskin MB (1994) Expression of neuron-specific tubulin defines a novel population in the proliferative layers of the developing telencephalon. J Neurosci 14:5399–5416

Meyer G, Wahle P (1999) The paleocortical ventricle is the origin of reelin-expressing neurons in the marginal zone of the foetal human neocortex. Eur J Neurosci 11:3937–3944

Meyer G, Schaaps JP, Moreau L, Goffinet AM (2000) Embryonic and early fetal development of the human neocortex. J Neurosci 20:1858–1868

Meyer G, Soria JM, Martinez-Galan JR, Martin-Clemente B, Fairen A (1998a) Different origins and developmental histories of transient neurons in the marginal zone of the fetal and neonatal rat cortex. J Comp Neurol 397:493–518

Miyata T, Kawaguchi A, Okano H, Ogawa M (2001) Asymmetric inheritance of radial glial fibers by cortical neurons. Neuron 31:727–741

Miyata T, Kawaguchi A, Saito K, Kawano M, Muto T, Ogawa M (2004) Asymmetric production of surface-diving and non surface-dividing cortical progenitor cells. Development 131(13): 3133–3145

Mollgard K, Schumacher U (1993) Immunohistochemical assessment of cellular proliferation in the developing human CNS using formalin-fixed paraffin-embedded material. J Neurosci Methods 46:191–196

Monier A., Evrard P., Gressens P., Verney C. (2006) Distribution and differentiation of microglia in the human encephalon during the first two trimesters of gestation. J. Comp Neurol 499:565–582

Nery S, Wichterle H, Fishell G (2001) Sonic hedgehog contributes to oligodendrocyte specification in the mammalian forebrain. Development 128:527–540

Nery S, Corbin JG, Fishell G (2003) Dlx2 progenitor migration in wild type and Nkx2.1 mutant telencephalon. Cereb Cortex 13:895–903

Noctor SC, Martinez-Cerdeno V, Ivic L, Kriegstein AR (2004) Cortical neurons arise in symmetric and asymmetric division zones and migrate through specific phases. Nat Neurosci 7:136–144

Noctor SC, Flint AC, Weissman TA, Dammerman RS, Kriegstein AR (2001) Neurons derived from radial glial cells establish radial units in neocortex. Nature 409:714–720

Noctor SC, Flint AC, Weissman TA, Wong WS, Clinton BK, Kriegstein AR (2002) Dividing precursor cells of the embryonic cortical ventricular zone have morphological and molecular characteristics of radial glia. J Neurosci 22:3161–3173

Nowakowski RS, Lewin SB, Miller MW (1989) Bromodeoxyuridine immunohistochemical determination of the lengths of the cell cycle and the DNA-synthetic phase for an anatomically defined population. J Neurocytol 18:311–318

O'Rahilly RMF (1999) The embryonic human brain: an atlas of developmental stages. Wiley-Liss, New York

Parnavelas JG (2000) The origin and migration of cortical neurones: new vistas. Trends Neurosci 23:126–131

Perez Villegas EM, Olivier C, Spassky N, Poncet C, Cochard P, Zalc B, Thomas JL, Martinez S (1999) Early specification of oligodendrocytes in the chick embryonic brain. Dev Biol 216:98–113

Polkinghorne report; Committee to Review the Guidance on the Research Use of Fetuses and Fetal Material. Review of the guidance on the research use of fetuses and fetal material (Her Majesty's Stationery Office, London, 1989)

Privat A (1975) Postnatal gliogenesis in the mammalian brain. Int Rev Cytol 40:281–323

Qian X, Shen Q, Goderie SK, He W, Capela A, Davis AA, Temple S (2000) Timing of CNS cell generation: a programmed sequence of neuron and glial cell production from isolated murine cortical stem cells. Neuron 28:69–80

Quinn, J.C., Molinek, M., Martynoga, B.S., Zaki, P.A., Faedo, A., Bulfone, A., Hevner RF, West JD, Price DJ (2006) Pax6 controls cerebral cortical cell number by regulating exit from the cell cycle and specifies cortical cell identity by a cell autonomous mechanism. Develop Biol. doi:10.1016.i.vdbio 2006.08.035

Raedler E, Raedler A (1978) Autoradiographic study of early neurogenesis in rat neocortex. Anat Embryol (Berl) 154:267–284

Rakic P (1972) Mode of cell migration to the superficial layers of fetal monkey neocortex. J Comp Neurol 145:61–83

Rakic P (1974) Neurons in rhesus monkey visual cortex: systematic relation between time of origin and eventual disposition. Science 183:425–427

Rakic S, Zecevic N (2003) Emerging complexity of layer I in human cerebral cortex. Cereb Cortex 13:1072–1083

Rezaie P, Dean A, Male D, Ulfig N (2005) Microglia in the cerebral wall of the human telencephalon at second trimester. Cereb Cortex 15:938–949

Rickmann M, Chronwall BM, Wolff JR (1977) On the development of non-pyramidal neurons and axons outside the cortical plate: the early marginal zone as a pallial anlage. Anat Embryol (Berl) 151:285–307

Sauer FC (1935a) The cellular structure of the neural tube. J Comp Neurol 63:13–23

Sauer FC (1935b) Mitosis in the neural tube. J Comp Neurol 62:377–405

Sauer FC, Walker BE (1959) Radiographic study of interkinetic nuclear migration in the neural tube. Proc Soc Exp Biol Med 101:557–560

Simonati A, Tosati C, Rosso T, Piazzola E, Rizzuto N (1999) Cell proliferation and death: morphological evidence during corticogenesis in the developing human brain. Microsc Res Tech 45:341–352

Smart IH (1973) Proliferative characteristics of the ependymal layer during the early development of the mouse neocortex: a pilot study based on recording the number, location and plane of cleavage of mitotic figures. J Anat 116:67–91

Smart IH (1985) A localised growth zone in the wall of the developing mouse telencephalon. J Anat 140(Pt 3):397–402

Smart IH, Smart M (1977) The location of nuclei of different labelling intensities in autoradiographs of the anterior forebrain of postnatal mice injected with [3H]thymidine on the eleventh and twelfth days post-conception. J Anat 123:515–525

Smart IH, McSherry GM (1982) Growth patterns in the lateral wall of the mouse telencephalon. II. Histological changes during and subsequent to the period of isocortical neuron production. J Anat 134(Pt 3):415–442

Smart IH, Dehay C, Giroud P, Berland M, Kennedy H (2002) Unique morphological features of the proliferative zones and postmitotic compartments of the neural epithelium giving rise to striate and extrastriate cortex in the monkey. Cereb Cortex 12:37–53

Stewart GR, Pearlman AL (1987) Fibronectin-like immunoreactivity in the developing cerebral cortex. J Neurosci 7:3325–3333

Sturrock RR, Smart IH (1980) A morphological study of the mouse subependymal layer from embryonic life to old age. J Anat 130:391–415

Suzuki H, Franz H, Yamamoto T, Iwasaki Y, Konno H (1988) Identification of the normal microglial population in human and rodent nervous tissue using lectin immunohistochemistry. Neuropathol Appl Neurobiol 14(3):221–227

Takahashi T, Nowakowski RS, Caviness VS Jr (1993) Cell cycle parameters and patterns of nuclear movement in the neocortical proliferative zone of the fetal mouse. J Neurosci 13:820–833

Takahashi T, Nowakowski RS, Caviness VS Jr (1995) Early ontogeny of the secondary proliferative population of the embryonic murine cerebral wall. J Neurosci 15:6058–6068

Tamamaki N, Nakamura K, Okamoto K, Kaneko T (2001) Radial glia is a progenitor of neocortical neurons in the developing cerebral cortex. Neurosci Res 41:51–60

Tiu SC (2001) Development of the human cortex. A neuroanatomical and histochemical study. MD thesis, Chinese University, Hong Kong

Valverde F, De Carlos JA, Lopez-Mascaraque L (1995) Time of origin and early fate of preplate cells in the cerebral cortex of the rat. Cereb Cortex 5:483–493

Weissman T, Noctor SC, Clinton BK, Honig LS, Kriegstein AR (2003) Neurogenic radial glial cells in reptile, rodent and human: from mitosis to migration. Cereb Cortex 13:550–559

Wu CH, Wen CY, Shieh JY, Ling EA (1993) A quantitative study of the differentiation of microglial cells in the developing cerebral cortex in rats. J Anat 182(Pt 3):403–413

Wu SX, Nakamura K, Nakamura K, Kometani K, Minato N, Miyazaki S, Goebbels S, Nave KA, Kaneko T, Tamamaki N (2003) Pyramidal neuron production in the extraventricular zone of the mouse neocortex. In: 33rd Annual Society for Neuroscience. New Orleans, USA

Zecevic N (1993) Cellular composition of the telencephalic wall in human embryos. Early Hum Dev 32:131–149

Zecevic N (2004) Specific characteristic of radial glia in the human fetal telencephalon. Glia 48:27–35

Zecevic N, Milosevic A (1997) Initial development of gamma-aminobutyric acid immunoreactivity in the human cerebral cortex. J Comp Neurol 380:495–506

Zecevic N, Andjelkovic A, Matthieu JM, Tosic M (1998) Myelin basic protein immunoreactivity in the human embryonic CNS. Brain Res Dev Brain Res 105:97–108

Zecevic N, Chen Y, Filipovic R (2005) Contributions of cortical subventricular zone to the development of the human cerebral cortex. J Comp Neurol 491:109–122